Electronic Supplementary Material (ESI) for Journal of Materials Chemistry C.
This journal is © The Royal Society of Chemistry 2021

**Supporting Information**

# The novel mechanism in understanding a strong enhancement of photoluminescence quantum yield in large-area monolayer $MoS_2$ grown by CVD

Kishore K. Madapu,*[a] C. Abinash Bhuyan,[a] S. K. Srivastava,[b] and Sandip Dhara*[a]

Email: madupu@igcar.gov.in, dhara@igcar.gov.in

[a.] Surface and Nanoscience Division, Indira Gandhi Centre for Atomic Research, Homi Bhabha National Institute, Kalpakkam-603 102, India

[b.] Materials Physics Division, Indira Gandhi Centre for Atomic Research, Kalpakkam-603 102, India

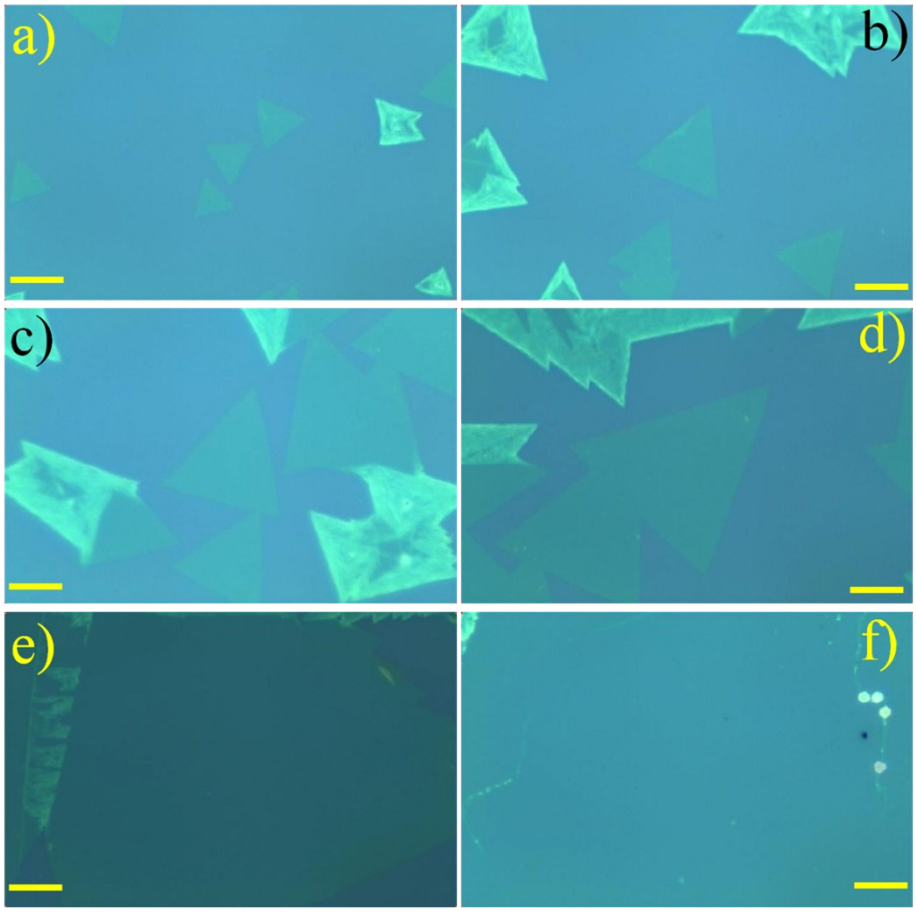


Figure S1. (a-d) Optical micrographs of $MoS_2$ monolayer structures grown on Si(300 nm)/Si. (e, f) A grain-free large area of $MoS_2$ monolayers. The scale shown in the figures corresponds to 10 μm.

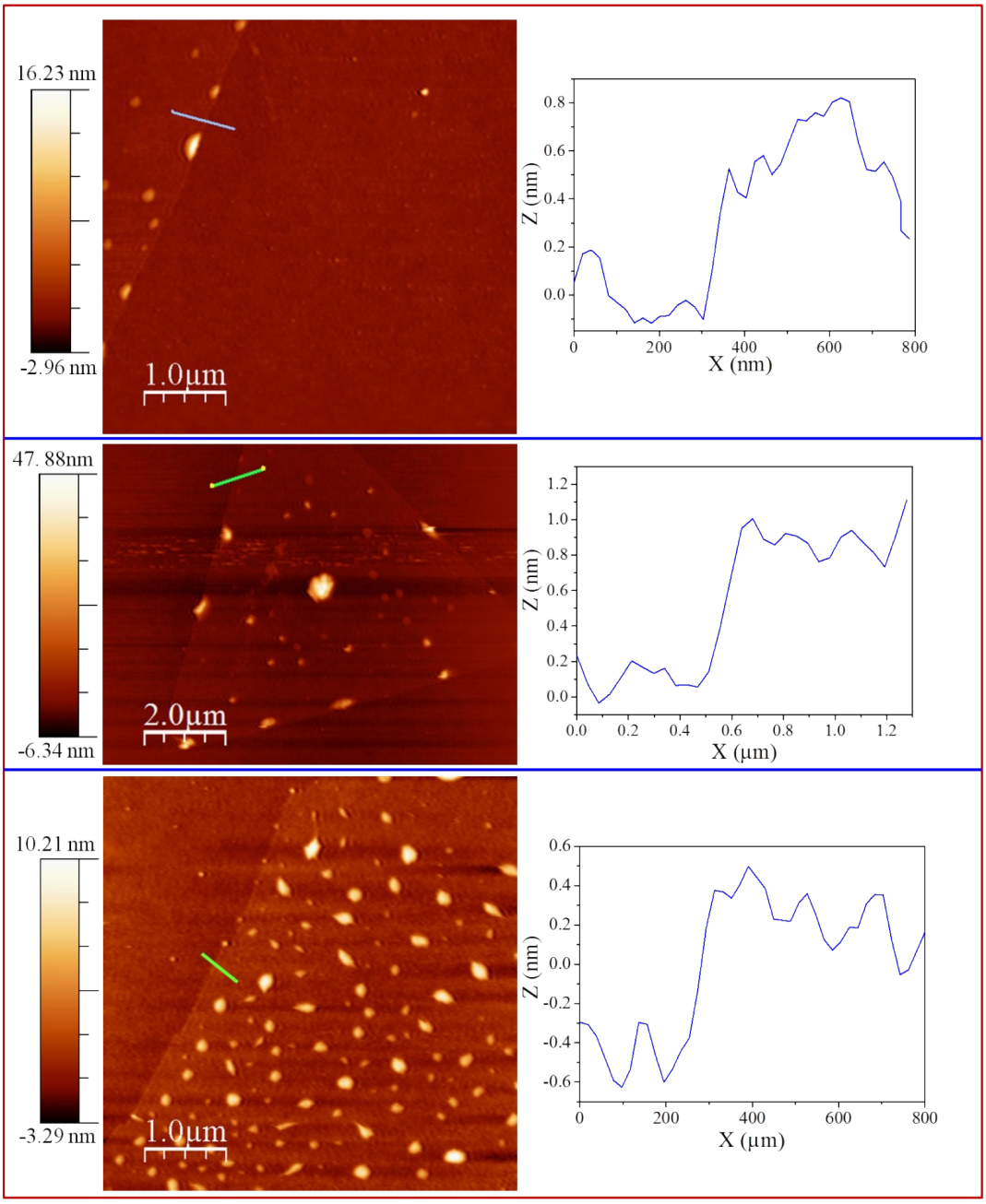


Figure S2. AFM topography analyses showing the thickness of the $MoS_2$ layers less than 0.9 nm confirming the formation of a monolayer.

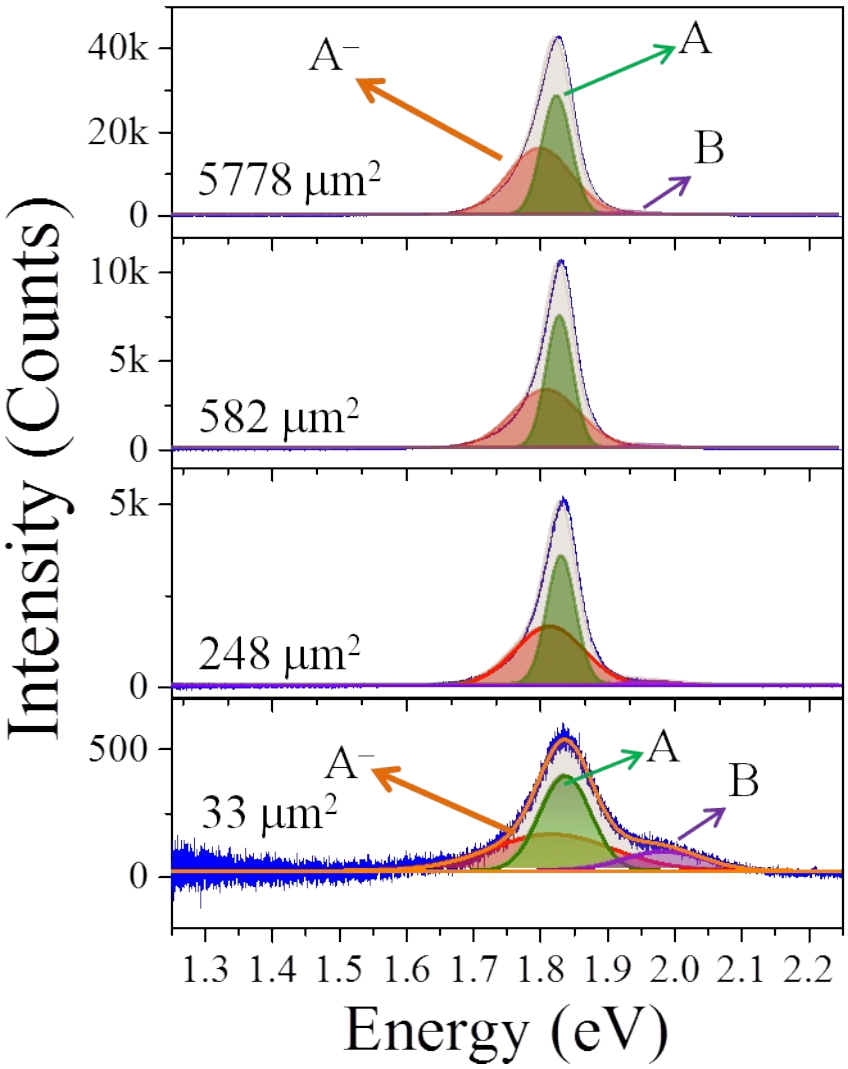


Figure S3. PL spectra of monolayer $MoS_2$ with different areas fitted with Gaussian functions.

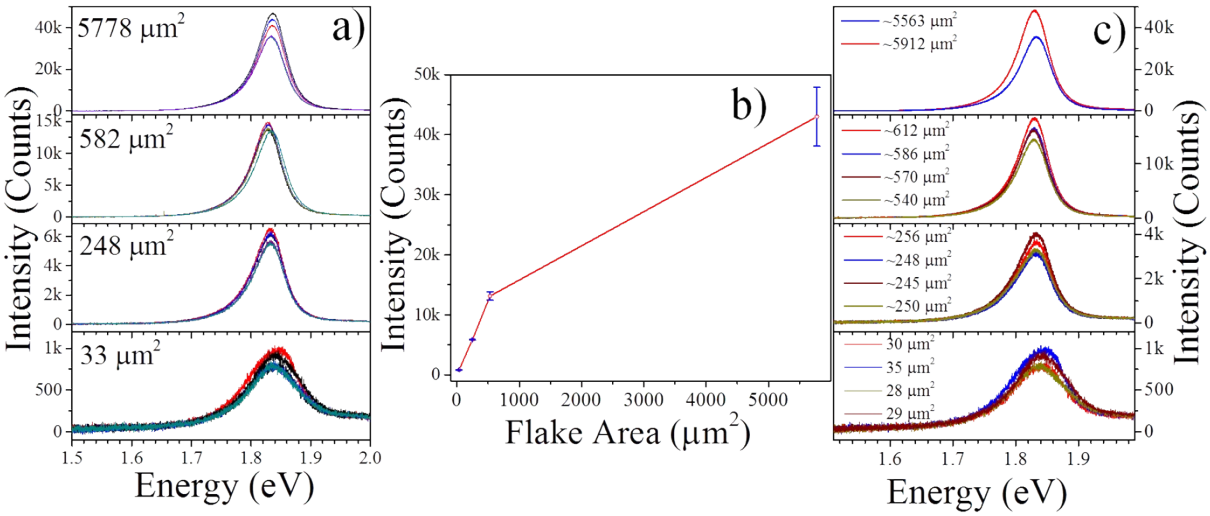


Figure S4**.** a) PL spectra collected at each flake area at different locations around the centre region. b) Variation of mean PL intensity with flake area. c) PL spectra collected at arbitrary flakes with the equivalent area.

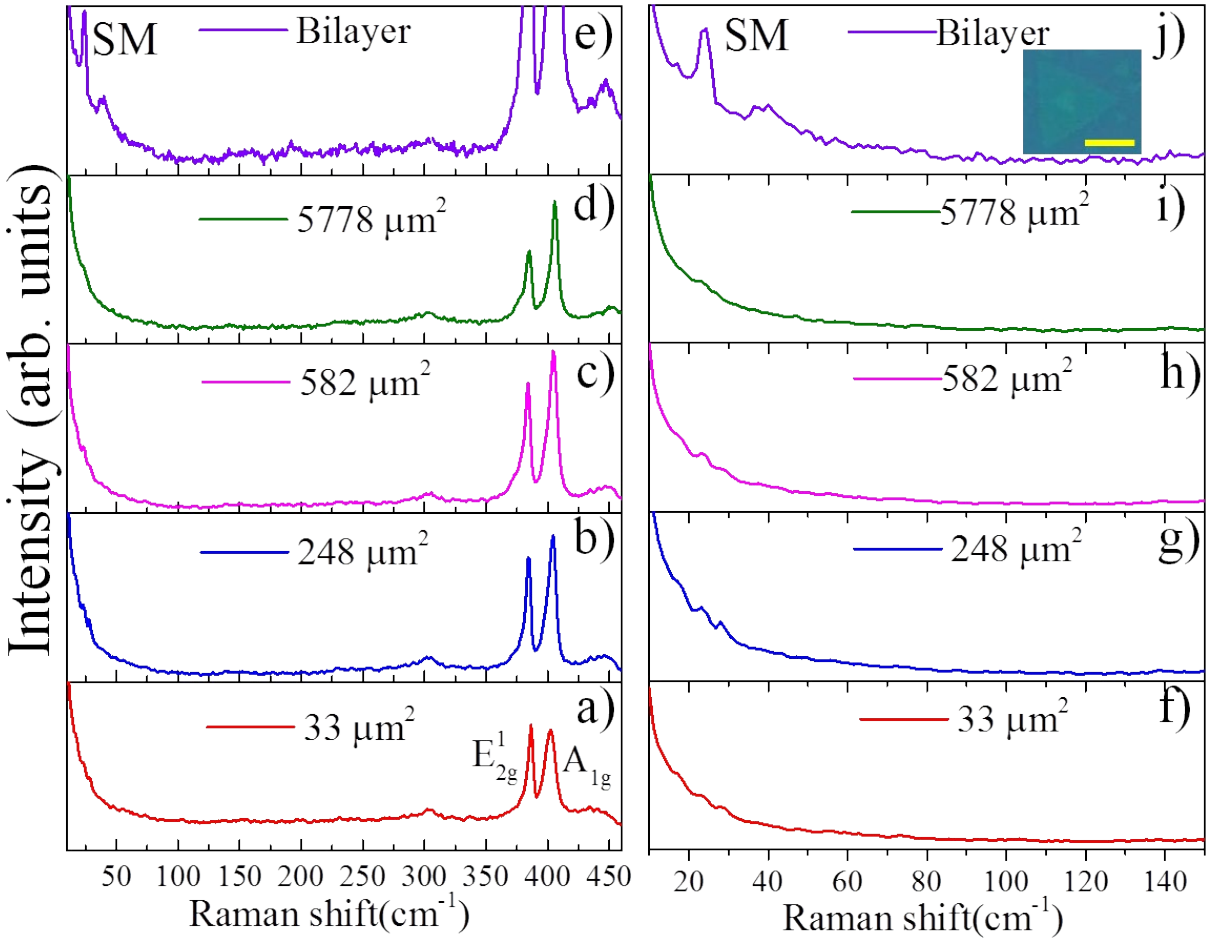


Figure S5. (a)-(d) Raman spectra of the 1L-$MoS_2$ flakes with varying sizes (area) and (f)-(i) corresponding zoomed low-frequency region, respectively. (e) Raman analyses of the bilayer $MoS_2$ flakes and (j) corresponding zoomed low-frequency region. The optical image of the bilayer structure is shown in the inset of (j) and the scale shown in the figure corresponds to the 5 μm.

The absence of the shear mode (SM) in all 1L-$MoS_2$ flakes (a-d) reveals that the flakes are monolayer structures. For comparison, bilayer $MoS_2$ shows the SM mode (e and j) in the Raman spectra. The low-frequency region is zoomed (f-i) to show a clear absence of SM mode for monolayer flakes.

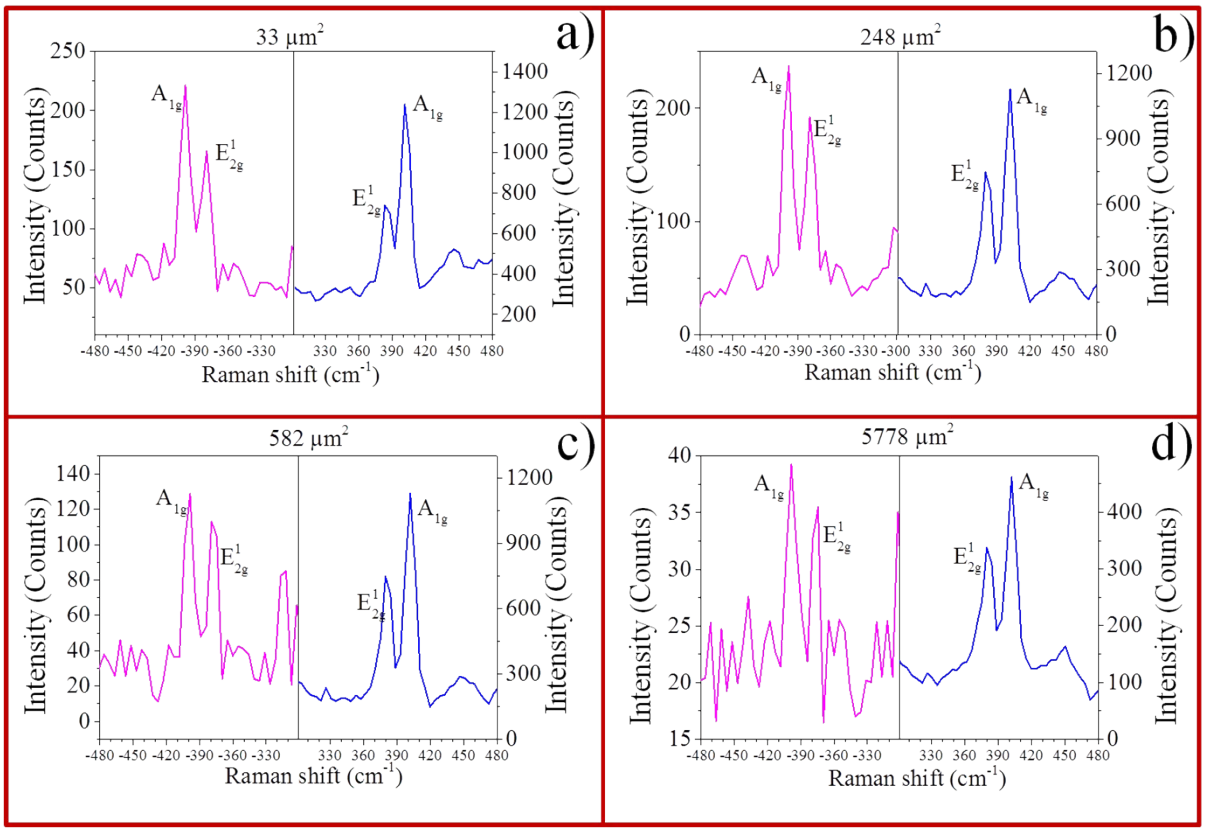


Figure S6. Stokes and anti-Stokes Raman spectra of $MoS_2$ monolayers with different areas.

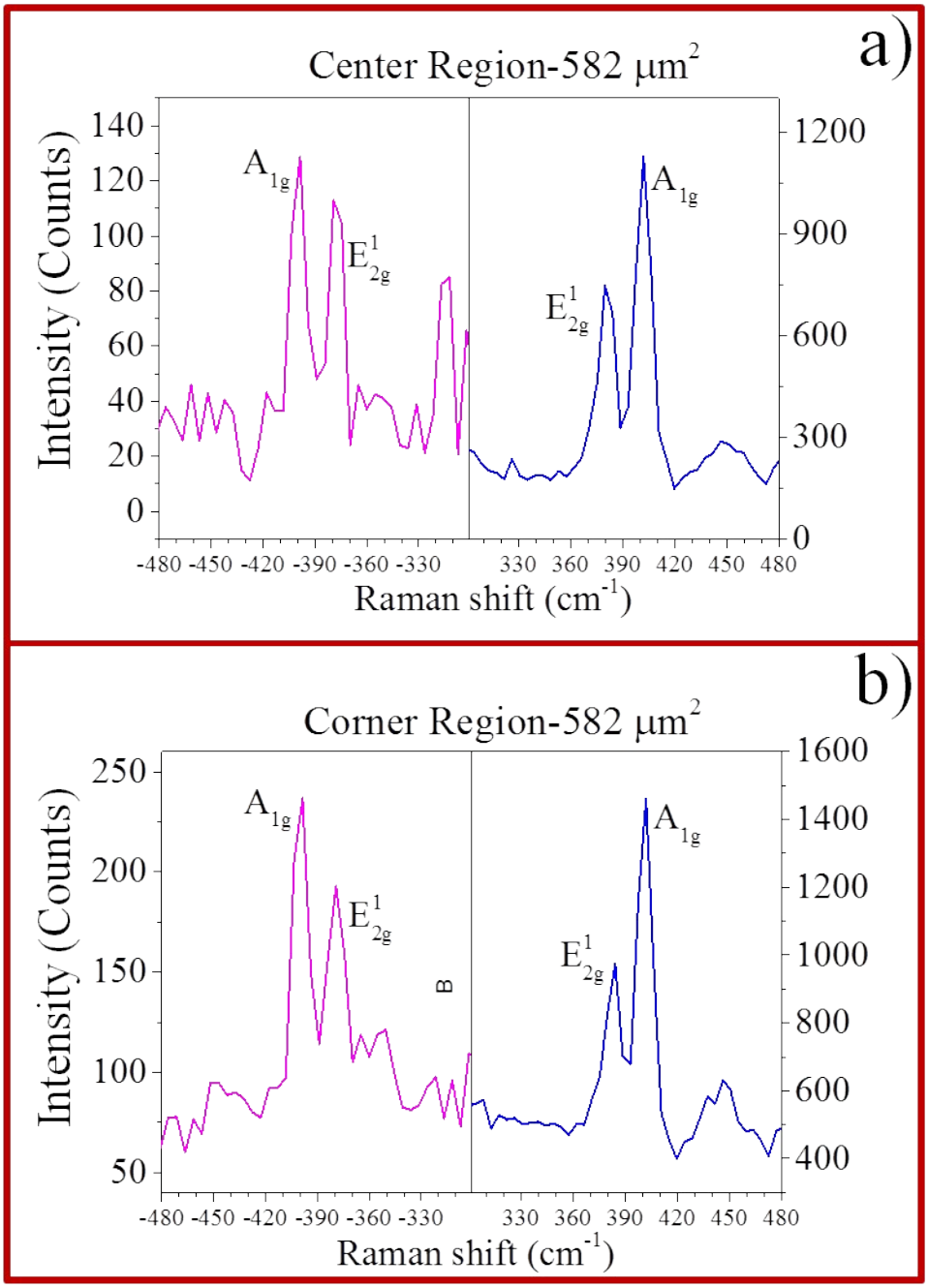


Figure S7. Stokes and anti-Stokes Raman spectra of $MoS_2$ monolayer flake (~582 μm$^2$) collected at (a) Center Region and (b) Corner Region.

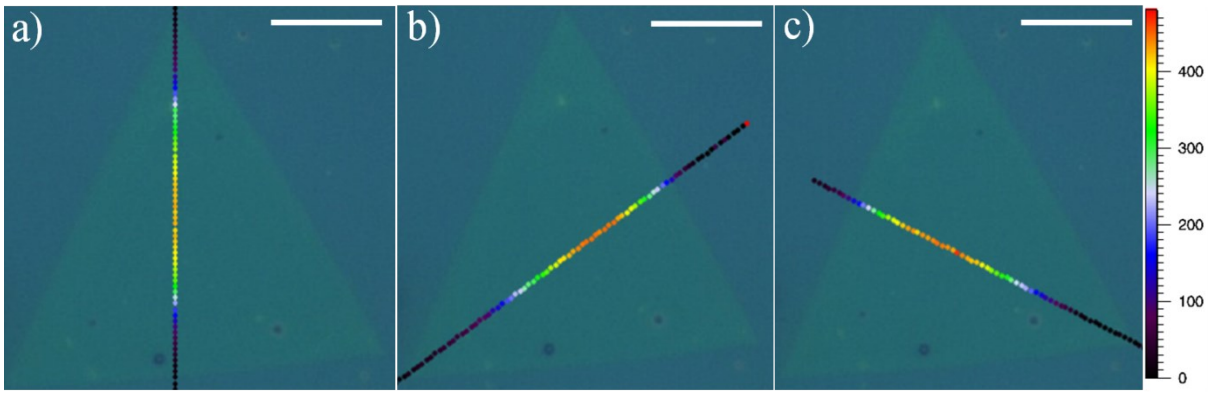


Figure S8. a)-c) Line imaging of PL peak intensity along the medians of triangular flake.

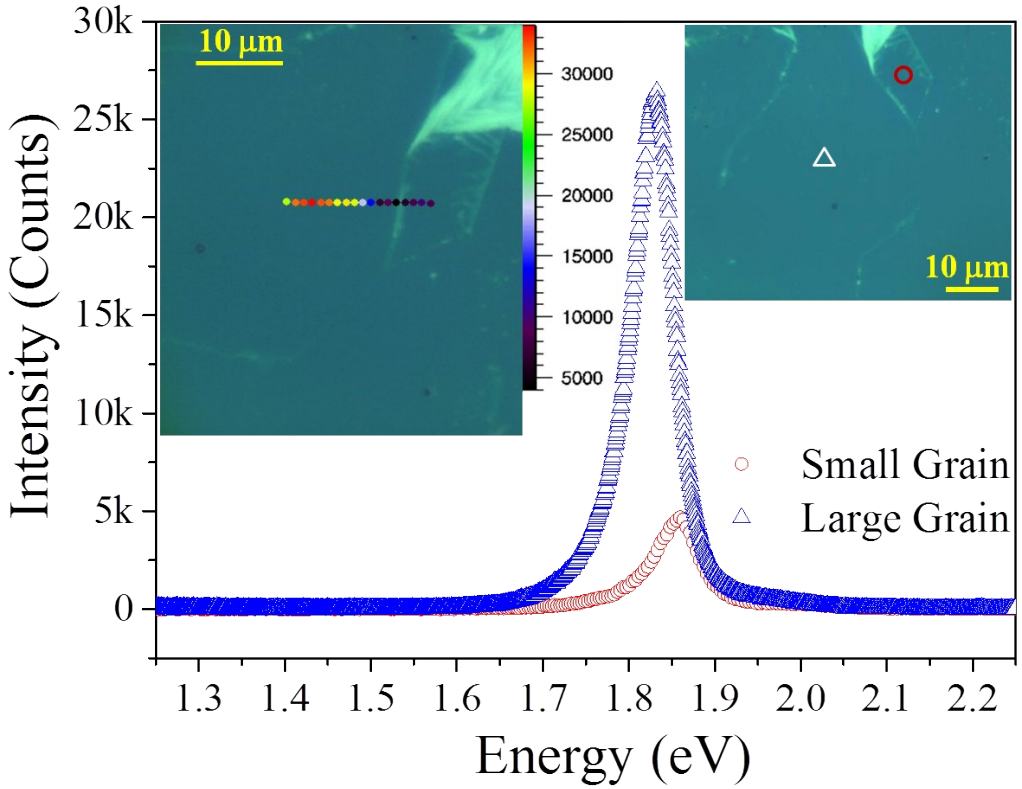


Figure S9. Typical PL spectra of 1L-$MoS_2$ collected from the large (~2663 µm$^2$) and small (~135 µm$^2$) grains. The centres of the collected regions are indicated by open triangle and circle in the optical micrograph, respectively (right hand side inset). PL line image is shown covering the part of the large and small grains (left side inset).

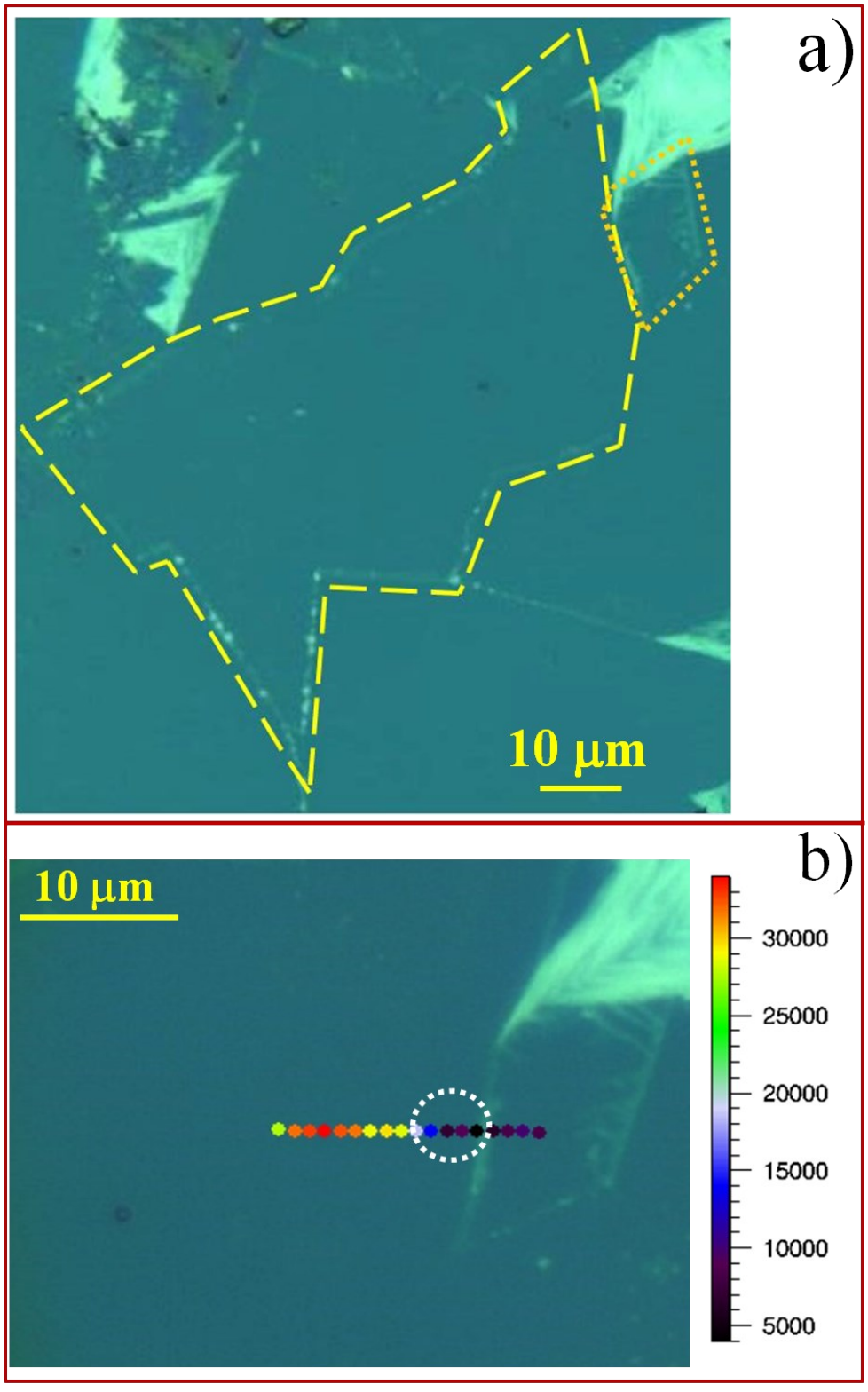


Figure S10. a) Optical micrograph of PL imaging area showing large grain and small grain with dashed and dotted boundaries, respectively. b) PL line image is shown covering the part of the large and small grains. PL intensity reduction near the grain boundary region indicated by a dotted ellipse.

**Table S1:** Peak position and intensities of A exciton and trion, the difference in the peak positions, and calculated carrier density values of each flake area. The values are extracted using the Gaussian fits of PL spectra.

| Area $\mu m^2$ | $P(A^-)$ eV | $I$(A-) | $P$(A) eV | $I$(A) | $P$(B) eV | $I$(A) | $D$(A-$A^-$) meV | $I$(A)/$I(A^-)$ | $n_e$ $\times 10^{13}$ $cm^{-2}$ |
|---|---|---|---|---|---|---|---|---|---|
| 33 | 1.816 | 32.15 | 1.837 | 35.46 | 1.983 | 11.02 | 21 | 1.103 | 2.76 |
| 248 | 1.813 | 210.72 | 1.834 | 189.90 | 1.966 | 12.13 | 21 | 0.901 | 2.25 |
| 532 | 1.811 | 414.67 | 1.831 | 373.75 | 1.965 | 13.27 | 20 | 0.901 | 2.25 |
| 5778 | 1.802 | 1915.64 | 1.827 | 1578.27 | 1.936 | 61.25 | 25 | 0.824 | 2.06 |

*P*-Position of the peak; *I*-Integrated intensity of peak; *D*-Difference in the peak positions of the A-exciton (A) and trion ($A^-$); $n_e$-Carrier density